Available online at www.sciencedirect.com
SCIENCE DIRECT
Polymer 46 (2005) 7896–7908
polymer
www.elsevier.com/locate/polymer

Gel electrolyte membranes derived from co-continuous polymer blends

Anette Munch Elmér, Patric Jannasch*

Department of Polymer Science and Engineering, Lund University, P.O. Box 124, SE-221 00 Lund, Sweden

Received 21 March 2005; received in revised form 20 June 2005; accepted 21 June 2005
Available online 27 July 2005

Abstract

Polymer gel electrolyte membranes were prepared by first casting films of poly(vinylidene fluoride-*co*-hexafluoropropylene) (PVDF–HFP), lithium bis(trifluoromethanesulfonyl)imide (LiTFSI) salt, and poly(ethylene glycol) (PEG) monomethacrylate and dimethacrylate macromonomers. Polymerization of the macromonomers initiated by UV-irradiation then generated solid films having phase-separated morphologies with a microporous PVDF–HFP phase embedded in PEG-grafted polymethacrylates. Gel electrolyte membranes were finally prepared by allowing the films to take up solutions of LiTFSI in γ-butyrolactone (γ-BL). The PEG-grafted polymethacrylate in the membranes was found to host the largest part of the liquid electrolyte, giving rise to a highly swollen ionic conductive phase. Results by FTIR spectroscopy showed that the Li^+ ions preferentially interacted with the ether oxygens of the PEG chains. The properties of the membranes were studied as a function of the ratio of PVDF–HFP to PEG-grafted polymethacrylate, as well as the degree of crosslinking, LiTFSI concentration, and liquid electrolyte content. The self-supporting and elastic gel membranes had ionic conductivities of 10^{-3} S cm^{-1} and a mechanical storage modulus in the range of 2.5 MPa in the tension mode at room temperature. Variation of the salt concentration showed the greatest effect on the membrane properties.

Keywords: Polymer gel electrolytes; Interpenetrating polymer blend networks; Vinylidene fluoride copolymers

1. Introduction

Since the 1970s, polymer electrolytes have received great attention for their potential application as electrolytes in rechargeable lithium batteries, electrochromic windows and sensors. However, despite years of extensive studies, solid polymer electrolytes have so far not achieved conductivities high enough to be widely used as battery electrolytes. Solid polymer electrolytes typically show conductivities below 10^{-5} S cm^{-1} at room temperature, while the requirement for applications in lithium batteries is a least 10^{-3} S cm^{-1}. Conductivities in this range can be reached by preparing polymer gel electrolytes. These electrolytes are formed by swelling a suitable polymer with a liquid electrolyte, consisting of a lithium salt dissolved in an aprotic organic solvent with a high dielectric constant. When the solvent is present, the mobility in the system increases and, if the combination of solvent, salt and polymer is chosen carefully, a polymer gel electrolyte with a high ionic conductivity within a broad temperature interval is obtained. Several polymers, such as polyacrylonitrile [1,2], poly(methyl methacrylate) [3] poly(vinylidene fluoride) [4], have been investigated as components in gel electrolytes.

Generally, polymer gel electrolytes have to posses a high ionic conductivity while retaining a sufficient mechanical stability. These demands are difficult to combine as the ionic conductivity is promoted by the presence of large amounts of electrolyte solution, which in turn impairs the mechanical stability. This problem has at least partly been overcome by crosslinking [5,6], addition of nanofillers [7,8], or trapping the solution in a microporous matrix [9–11]. A particular interest has been directed towards gel electrolytes with microporous matrices of vinylidene fluoride polymers, which may entrap various organic liquid electrolytes [9,10,12–14]. The porous polymer film provides the mechanical and dimensional stability, while the liquid electrolyte is the medium for the ionic conduction. The ability of the polymer to absorb and retain the electrolyte solution is crucial for the polymer gel electrolytes. Solvent loss can occur by leakage or evaporation. Thus, the affinity between

* Corresponding author. Tel.: +46 46 2229860; fax: +46 46 222 41 15.
E-mail address: patric.jannasch@polymer.lth.se (P. Jannasch).

0032-3861/$ - see front matter © 2005 Published by Elsevier Ltd.
doi:10.1016/j.polymer.2005.06.079

the polymer and liquid electrolyte is important for the solvent retention. Advantageously, polymers with a low degree of crystallinity are used. The solvent is then taken up by the amorphous parts of the polymer. Methods to reduce solvent leakage in polymer gel electrolytes include covering microporous membranes with solvent-retaining polymers [15,16], or preparing copolymers having segments with a high solvent retention [17].

In a previous study, we have prepared and investigated solid polymer electrolytes based on co-continuous polymer blends of poly(vinylidene fluoride-*co*-hexafluoropropylene) (PVDF–HFP) and poly(methacrylate)s grafted with short poly(ethylene glycol) (PEG) side chains hosting lithium bis(trifluoromethanesulfonyl)imide (LiTFSI) salt [18]. These electrolytes were found to have a morphology consisting of microporous PVDF–HFP phases incorporated in continuous networks of amorphous PEG-grafted polymethacrylates. They further possessed a good mechanical stability, a thermal stability below 140 °C, and showed a conductivity of 10^{-5} S cm^{-1} at room temperature. In order to increase the conductivity, and to study the influence of additions of liquid electrolytes, we have in the present study prepared gel membranes by allowing the solid dry membranes to take up controlled amounts of electrolyte solution. These gel membranes were investigated with regard to ionic conductivity, and thermal and mechanical properties.

2. Experimental

2.1. Materials

PEG monomethacrylate macromonomer (PEG400mMA, having PEG chain segments of $M_n = 400$ g mol^{-1}) and PEG dimethacrylate macromonomer (PEG400diMA, $M_n = 400$ g mol^{-1}) were obtained from Polysciences and Aldrich, respectively. PVDF–HFP (Kynar Flex® 2801, Elf Atochem Inc., 88 wt% vinylidene difluoride) was dried in vacuum at 100 °C for 24 h prior to use. Acetone (p.a) and the UV-activator 2,2-dimethoxy-2-phenylacetophenone (99%) was obtained from Fisher Chemicals and Aldrich, respectively. LiTFSI salt (battery grade) was kindly supplied by the 3M Company. All chemicals except PVDF–HFP were used as received, and were stored and handled in an argon filled glove box to avoid water and oxygen contact.

2.2. Preparation of dry membranes

The details concerning the preparation of the solid membranes have been described previously [18]. In summary, films were cast from acetone solutions of PVDF–HFP, PEG methacrylate macromonomers, LiTFSI, and the UV-activator. After drying, polymerization of the macromonomers was initiated by UV-irradiation. All handling was performed in the argon filled glove box. By using this procedure, self-standing and slightly opaque solid membranes with varying amount of PVDF–HFP content, and degrees of crosslinking within the PEG phase were obtained, see Scheme 1. These dry solid samples were approximately 300–600 μm thick, and were designated PEG$x-y$, where x indicated the total wt% of the PEG macromonomer mixture, PEG400diMA and PEG400mMA in the samples, and y the wt% of dimethacrylate in the PEG macromonomer mixture. The combined PEG macromonomer content was kept at 70, 80, 85, and 100 wt%, while the degree of crosslinking in the PEG phase was varied by adding PEG400diMA corresponding to 0, 2, 5, and 10 wt% of the combined PEG macromonomer mixture. The ratio of ether oxygens to Li^+ ions was kept at 31:1 in all samples.

2.3. Microscopy

Scanning electron microscopy (SEM) was employed in order to study the morphology of the supporting PVDF–HFP phase. After film casting, pieces of solid membranes without the crosslinker PEG400diMA were immersed into distilled water for 24 h to leach out the PEG macromonomers. After subsequent drying, the samples were sputter-coated with a 15 nm thick layer of Pt before studying the external surfaces exposed to either argon or glass during casting, and internal surfaces exposed after cryo-fracture of the leached samples in liquid nitrogen. The study was performed using an ISI 100A scanning electron microscope.

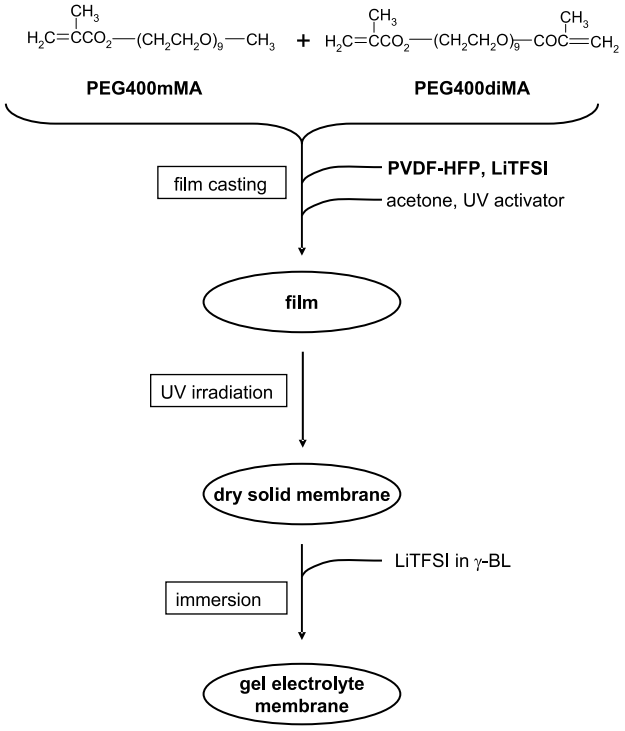

Scheme 1. Preparation of polymer gel electrolyte membranes consisting of PVDF–HFP networks hosting crosslinked PEG-grafted methacrylates swollen by solutions of LiTFSI in γ-BL.

2.4. Evaluation of equilibrium swelling

The equilibrium swelling was measured after immersing dry solid membranes in a solution of 1.0 M LiTFSI in γ-BL for 24 h. The swollen membranes were then taken out of the solution, carefully dried using tissue paper, and weighed. The equilibrium swelling of the samples was subsequently calculated as:

$$w_s^{eq} = (m_g - m_0)m_g^{-1} \times 100\% \quad (1)$$

where w_s^{eq} was the equilibrium swelling, m_0 was the weight of the original dry solid sample, and m_g was the weight of the gel membrane after swelling.

2.5. Preparation of gel electrolyte membranes

Different gel membranes were prepared by immersing pieces of dry solid membranes in liquid electrolyte solutions, thereby allowing them to take up $w_s = 20$, 40, and 60 wt% liquid content. Solutions of 0, 0.5, 1.0, 1.5, and 2.0 M LiTFSI in γ-BL were used in the study. The samples were each immersed in the respective solution just long enough to take up the desired amount of electrolyte solution. Characterization of the gel membranes was performed within 15 min after the swelling procedure.

2.6. IR spectroscopy

The gel membranes were studied by over-head attenuated total reflectance Fourier transform infrared spectroscopy (ATR-FTIR) to investigate the chemical composition at the surface. Spectra were recorded using a Bruker IFS 66 spectrometer, using an ATR-unit with a zink selenide crystal reflecting at 45°. The spectral resolution was set to 4 cm^{-1}, and 200 scans were recorded for each sample.

2.7. Differential scanning calorimetry

The thermal properties of the gel membranes were investigated using a TA instruments DSC Q 1000. Pieces of membranes were loaded in aluminum pans inside the argon filled glove box. After hermetically sealing the pans, the samples were then placed in the DSC cell and cooled from room temperature to −150 °C and kept there for 3 min, followed by heating to 100 °C. After keeping this temperature for 1 min, the samples were cooled to 0 °C. All scans were performed at a rate of 10 °C min^{-1} under helium purge. The reported glass transition temperatures (T_g) were taken as the inflection point of ΔC_p measured during the heating scan.

2.8. Dynamic mechanical analysis

The mechanical properties of the gel membranes were evaluated by dynamic mechanical analysis (DMA) in the tension mode, using a TA instruments DMA 2980. The membranes were cut into rectangular pieces with a length and width of approximately 20 and 5 mm, respectively. Both ends of the rectangular samples were supported by aluminum foil to prevent membrane failure at the clamps. The storage modulus (E'), loss modulus (E''), and tan $\delta (= E''/E')$ were recorded in the temperature range −120 to 25 °C at a heating rate of 3 °C min^{-1}. The measurements were performed at a frequency of 1 Hz and an amplitude of 1 μm.

2.9. Conductivity measurements

The conductivity of the gel membranes was evaluated by electrochemical impedance spectroscopy (EIS) using a Novocontrol σ-high resolution dielectric analyzer with a Novocool Cryosystem. Circular pieces with a diameter of 8 mm were punched out from the membranes, and placed between two highly polished stainless steel blocking electrodes in a specially constructed measuring cell [18]. The air-tight cell was sealed inside the argon filled glove box, allowing the mounted membrane to be handled outside the glove box without risking contact with air or water. The impedance measurements were carried out in the frequency range from 10^7 to 10^{-1} Hz at a 0.5 V amplitude. Spectra were recorded at every 10 °C between −40 and 100 °C after equilibration for 60 s at each temperature. Data was presented in the complex (Z', $-Z''$) plane, and the bulk resistance (R_b) was taken from the frequency that produced the minimum imaginary response, see Fig. 1. The conductivity (σ) was finally calculated as:

$$\sigma = l(AR_b)^{-1} \quad (2)$$

where l and A are the sample thickness and area,

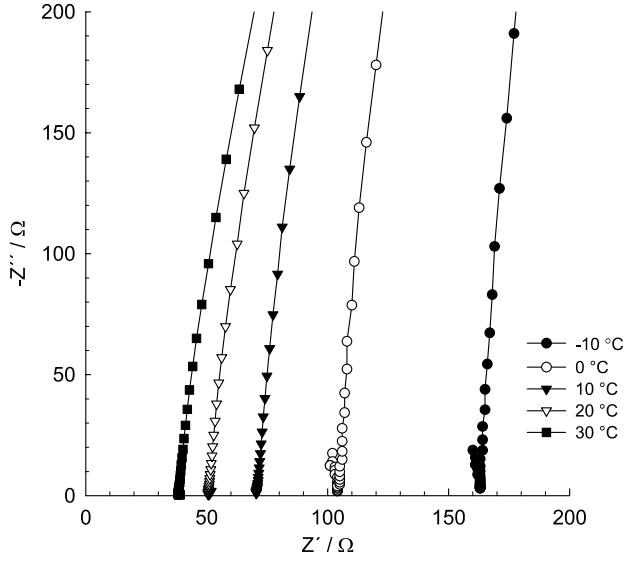

Fig. 1. Typical impedance response from the gel membranes. The plots show data collected for membrane PEG80-2 containing 60 wt% with 1.0 M LiTFSI in γ-BL.

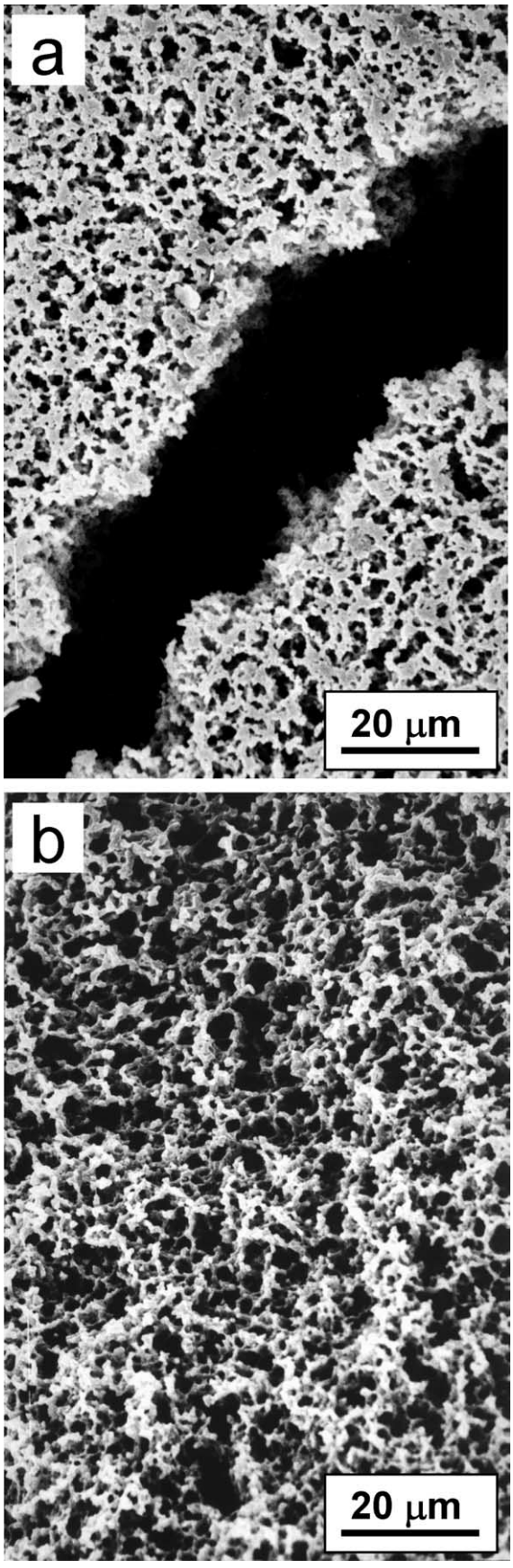

Fig. 2. SEM micrographs of the solid sample PEG85-0 where the PEG methacrylates have been leached out with water directly after casting the film. The micrographs show the remaining PVDF–HFP phase at (a) the surface exposed to argon during casting (a crack was deliberately introduced to expose the bulk morphology) and (b) the surface exposed after cryofracturing the sample, showing the bulk morphology.

respectively. The gel membranes were compressible and the precise dimensions of the circular samples during the impedance analysis was measured after dissembling the sample cell.

3. Results and discussion

3.1. Membrane preparation

Gel membranes were prepared from dry solid membranes, by allowing them to take up controlled amounts of γ-BL solutions of various salt concentrations, see Scheme 1. The gel membranes were all self-supporting, elastic and slightly opaque. The opacity was a consequence of the phase-separated morphology of the membranes. The structure of the PVDF–HFP phase in the solid membranes was studied under dry conditions by SEM. After the casting from acetone solutions, the PEG macromonomers were leached out by immersion in distilled water. Microscopy revealed a continuous PVDF–HFP phase with pores on the micron-scale, as shown by the micrographs of sample PEG85-0 in Fig. 2(a) and (b). It is highly desirable to have an open porous structure of the PVDF–HFP phase in the present membranes because the semicrystallinity of this phase is in principle a barrier to ionic conduction since PVDF–HFP takes no active part in the conduction process [19].

It was noted that an increased content of PVDF–HFP produced more elastic gel membranes, while a higher degree of crosslinking of the PEG-grafted methacrylate increased the fragility of the membranes. γ-BL has a melting point at −31 °C and a boiling point at around 205 °C which means that solvent evaporation can be restricted and that the thermal transitions of the polymer matrix in these gel membranes can be studied without any overlapping and disturbing transitions from the solvent.

3.2. Swelling of the membranes

The equilibrium swelling, w_s^{eq}, of the different solid samples in 1.0 M LiTFSI in γ-BL can be seen in Fig. 3. As expected, the highest degree of swelling was obtained for the solid membrane that contained the largest amount of PEG phase and had the lowest degree of crosslinking. Generally, two opposing effects control the degree of swelling of a polymer network to form a gel, namely the entropy (and possibly enthalpy) gain when mixing the

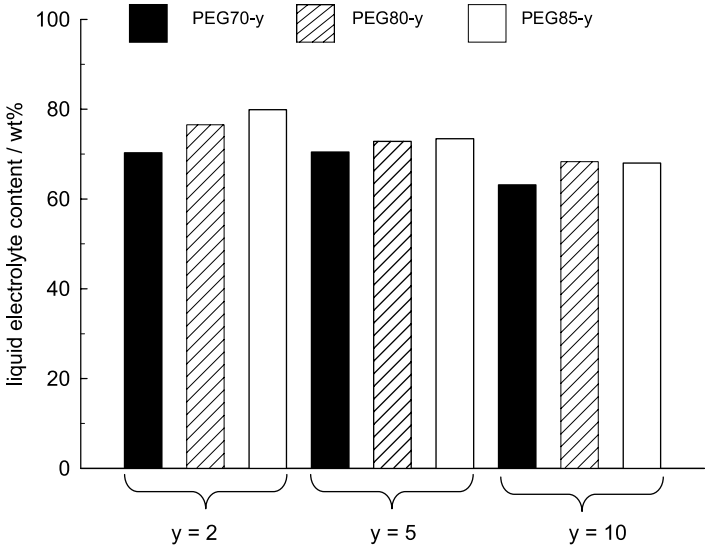

Fig. 3. Equilibrium swelling of membranes PEG$x-y$ containing 1.0 M LiTFSI in γ-BL at room temperature.

polymer network with the solvent, and the retractive force which increases when the polymer coil conformation deforms during solvent swelling [20]. A highly crosslinked network restricts the stretching of the polymer chains when the amount of solution increases during swelling, and thus opposes the deformation of the polymer network.

Although not directly measured, it was noted that the time required for the solid samples to take up 60 wt% liquid electrolyte content increased with the crosslink density in the PEG phase of the membranes. Also, increasing the salt concentration of the liquid electrolyte led to decreased swelling rates. The time required for samples to imbibe the solvent is reported to be proportional to the friction between the network and the solvent, where the friction can be viewed as the viscous interaction between the solvent and the polymer [21]. In the present case, the Li^+ ions in the electrolyte solutions have solvation shells of coordinating γ-BL molecules, and will thus constitute a much larger specie than the solvent molecules in the pure γ-BL. As the degree of crosslinking increases, the steric hindrance during the diffusion of the liquids will increase. Caillon-Caravanier et al. have studied the solubility of silica-filled PVDF–HFP in γ-valerolactone solutions with different concentrations of LiTFSI [22]. They found that an increase of the salt concentration decreased the rate of the swelling process which is in agreement with the findings in the present study.

Several factors favor a preferential swelling of the PEG phase by the electrolyte solution in the membranes. The PEG-grafted polymethacrylate phase can be expected to have a higher affinity for the liquid electrolyte, as compared to the PVDF–HFP phase, because of the presence of Lewis basic ether oxygens in the molecular structure which can interact with Li^+ ions. Alkali metal cations preferentially interact with the PEG chains [23,24], causing transient physical crosslinks [25] resulting from the coordination of Li^+ by the ether oxygens of the polymer [26]. These crosslinks restrict the molecular mobility of the PEG chains, giving rise to an increase in T_g. Furthermore, PVDF–HFP has a lower compatibility with neat γ-BL than PEG-based polymers. The former polymer is regarded as a 'low affinity polymer' for organic carbonates [27], and it is further reported that PVDF forms a gel with γ-BL by liquid–liquid phase separation followed by crystallization [28]. The crystalline regions of the PVDF–HFP can be assumed to be an impenetrable barrier for the solvent molecules and the solvent uptake therefore only takes place in the amorphous PVDF–HFP regions. Pure Kynar Flex 2801 is reported to take up 39 wt% of propylene carbonate at 30 °C [29], a solvent with a solubility parameter, 27 $(MPa)^{1/2}$, similar to that of γ-BL, 26 $(MPa)^{1/2}$ [30]. Experiments in our laboratory have shown that PVDF–HFP films only take up about 25 wt% of 1 M LiTFSI in γ-BL solution. From our previous study of the dry solid polymer electrolyte membranes, we showed that they exhibited a phase separated morphology with a microporous network embedded in a PEG phase as shown in Fig. 2 [18]. We also concluded that the PVDF–HFP phase consisted of spheroidal crystalline domains interconnected by fibrillar crystalline domains which were surrounded by regions of amorphous PVDF–HFP blended with PEG phase. Considering the discussion above, we concluded that the liquid electrolyte preferably interacted with the PEG-grafted methacrylate after selective swelling, leaving a more or less unaffected microporous PVDF–HFP phase. This implies that the present membranes have a higher solvent retention, as compared to corresponding gels without crosslinked PEG networks. Because of the selective uptake of the electrolyte solutions by the PEG phase, the present gel electrolytes must be regarded as quite complex multiphase systems with potential internal mechanical stresses between the phases.

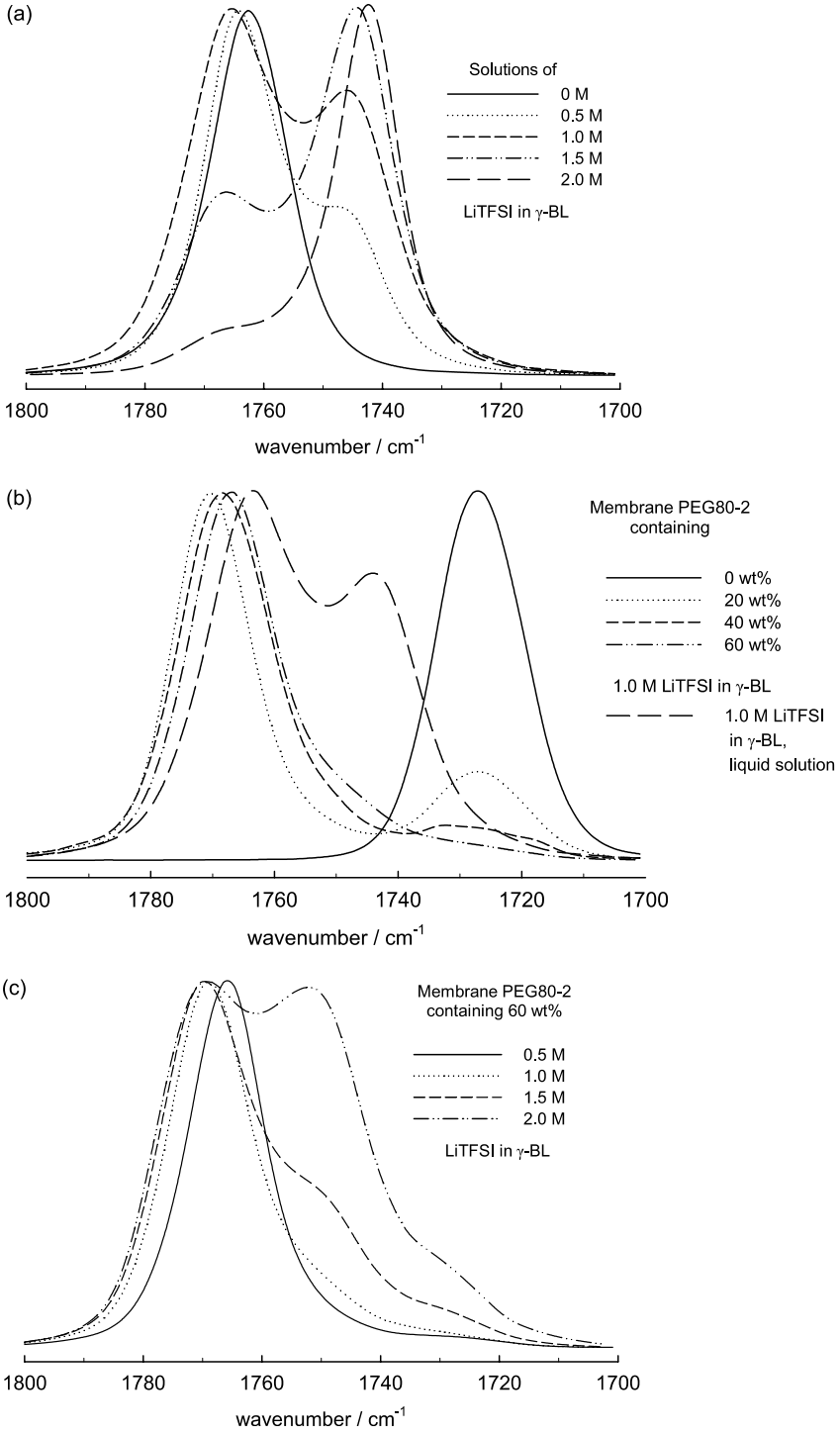

Fig. 4. FTIR spectra showing the carbonyl region of (a) liquid electrolyte solutions with varying LiTFSI salt concentration, (b) gel membranes based on membrane PEG80-2, with varying liquid electrolyte contents, and (c) gel membranes based on membrane PEG80-2 with varying salt concentrations.

3.3. Ionic interaction

FTIR spectroscopy is a very sensitive method for studying the local physical and chemical environment of chemical groups. This method was employed in the present study to investigate the state of the carbonyl groups in the gel membranes by observing changes in the carbonyl stretching band in the region 1870–1540 cm^{-1}. The carbonyl region of the neat γ-BL and liquid electrolyte solutions with different concentrations of LiTFSI in γ-BL is shown in Fig. 4(a). As seen, neat γ-BL showed a single absorption peak at 1760 cm^{-1}. After adding LiTFSI, a second peak appeared at 1745 cm^{-1}. The intensity of this peak increased with increasing salt concentration. Also, the

peak at 1760 cm^{-1} was slightly shifted towards higher wave numbers at higher LiTFSI concentrations. For the 1.5 and 2.0 M solutions, the peak at 1745 cm^{-1} was the dominating carbonyl band, indicating that it originated from γ-BL carbonyl groups coordinating Li^+ ions [31]. Using the density data from the study of Brouillette et al. on LiTFSI in γ-BL [32], the molar ratio of γ-BL:Li^+ was calculated to be 24:1, 11:1, 6:1, and 4:1 at 0.5, 1.0, 1.5, and 2.0 M, respectively. The solvation number of LiTFSI in γ-BL has been reported to be ~2:1 at a concentration close to 1 M [24].

Fig. 4(b) shows the carbonyl region of the gel membranes obtained by swelling the solid membrane PEG80-2 to different degrees with 1 M LiTFSI in γ-BL. The gel membranes showed a carbonyl peak at 1728 cm^{-1}, originating from the ester units of the PEG methacrylate networks. As expected, this peak decreased with increasing liquid electrolyte content because of dilution. The membrane containing 20 wt% liquid electrolyte still showed a significant absorption at 1728 cm^{-1}. However, the dominating peak was now observed at 1770 cm^{-1}, corresponding to the carbonyl groups of non-coordinating γ-BL. It was also noted that the position of the peak associated with the non-coordinating carbonyl groups of γ-BL shifted from 1770 down to 1765 cm^{-1} as the liquid electrolyte content was increased. Signs of coordinating carbonyl groups at higher liquid electrolyte contents were seen as a shoulder on the γ-BL peak extending toward 1745 cm^{-1}. The intensity of this shoulder increased with the amount of liquid electrolyte solution in the membranes.

Raman studies have previously shown that the cooperative coordination to the ether oxygens is highly preferred relative to the coordination of carbonates, and that cation–solvent interactions appear only when the PEG chains are saturated [33]. This is consistent with the results seen in Fig. 4(c), showing the carbonyl regions of the gel membranes obtained by swelling sample PEG80-2 to 60 wt% of electrolyte solutions of different salt concentrations. As expected, the absorption at 1745 cm^{-1} was the strongest for the membrane containing the 2.0 M solution.

3.4. Thermal properties

The thermal behavior of the gel membranes was studied by DSC. All membranes showed a glass transition related to the swollen PEG phase. Only the two membranes containing pure γ-BL and 0.5 M LiTFSI in γ-BL exhibited a cold crystallization, followed by melting transitions at around −50 °C during the heating scan, see Fig. 5. These transitions were related to γ-BL [34]. At higher salt concentrations, coordination of the Li^+ ions by γ-BL depressed the crystallization.

The dry solid membranes had T_gs of approximately −50 °C [18]. As seen in Table 1, the T_gs of the gel membranes varied between −122 and −71 °C depending on PEG phase content, degree of crosslinking, degree of swelling, and salt content. Gel membranes containing 60 wt% electrolyte solution showed an increase of T_g with their PEG content. This was most probably a consequence of the selective uptake of the liquid electrolyte in the PEG phase of the membranes. After liquid uptake, the membrane with lowest PEG content had the PEG phase with the highest degree of swelling, and thus the lowest T_g. Variation of the degree of covalent crosslinking within the PEG phase gave only minor changes in the T_g. Hence, the large degree of swelling of the PEG phase seemed to reduce the restrictions on polymer chain mobility set by the crosslinks. On the other hand, the salt concentration of the liquid electrolyte had a large impact, with increasing salt concentrations giving rise to increasing T_gs. The likely reason for this effect was an overall increasing degree of ionic interactions in the swollen PEG phase, and perhaps especially because of an increasing concentration of Li^+ ions coordinated by the ether oxygens of the PEG.

3.5. Dynamic mechanical properties

In order to investigate the mechanical properties of the gel membranes, they were subjected to oscillatory stress in the tension mode. The storage and loss modulus, E' and E'',

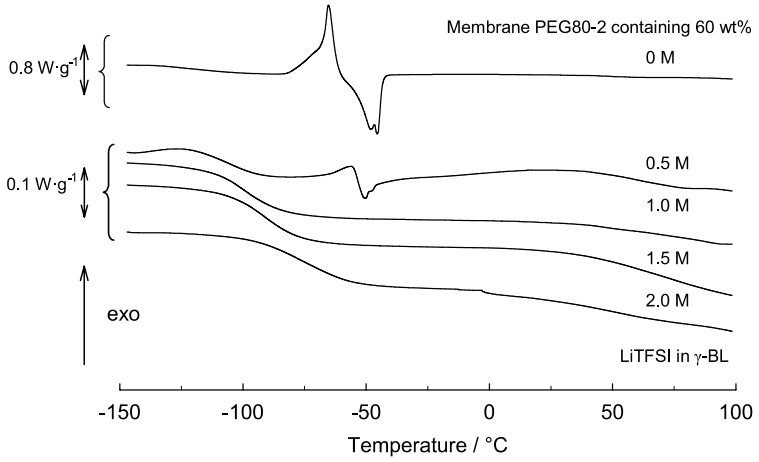

Fig. 5. DSC heating traces of gel membranes based on PEG80-2 containing 60 wt% electrolyte solutions with different LiTFSI salt concentrations.

Table 1
T_g of the gel membranes as evaluated by DSC

Membrane	Concentration of electrolyte solution in membrane (wt%)	LiTFSI concentration in γ-BL (M)	T_g (°C)
PEG70-2	60	1.0	−102
PEG80-2	60	1.0	−100
PEG85-2	60	1.0	−95
PEG80-2	60	1.0	−100
PEG80-5	60	1.0	−100
PEG80-10	60	1.0	−98
PEG80-2	60	0	−122
PEG80-2	60	0.5	−106
PEG80-2	60	1.0	−100
PEG80-2	60	1.5	−91
PEG80-2	60	2.0	−73
PEG80-2	20	1.0	−71
PEG80-2	40	1.0	−79
PEG80-2	60	1.0	−100

respectively, were measured as a function of temperature. A typical mechanical response of the samples is shown in Fig. 6. At −120 °C, E' and E'' were in the range of 10^3 and 10^2 MPa, respectively. During heating, the values of the modulii decreased significantly at the glass transition temperature of the swollen PEG phases. At 20 °C, E' of the gel membranes varied between 2 and 4 MPa. These values may be compared with those of the corresponding solid samples which exhibited values of E' between 3 and 15 MPa at 20 °C [18]. As expected, the gel membranes were mechanically stiffened by an increasing amount of PVDF–HFP, a higher degree of crosslinking, and an increased concentration of LiTFSI.

The position of the maximum of tan δ (tan δ_{max}) was related to the glass transition of the PEG phase containing the electrolyte solution. In the present study, the tan δ_{max} for the samples was found to be located approximately 15 °C higher than the T_g evaluated by DSC. An increase of the amount of the PEG phase in the membranes gave a decrease in the temperature at tan δ_{max}, see Fig. 7(a). This

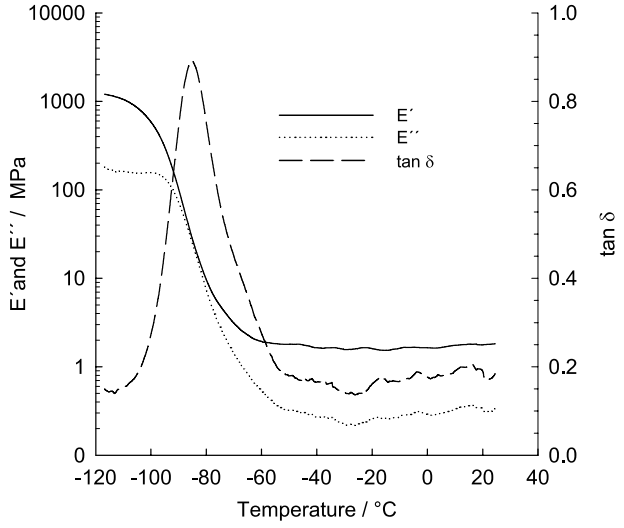

Fig. 6. DMA data of membrane PEG80-2 containing 60 wt% 0.5 M LiTFSI in γ-BL. The data was recorded in the tension mode.

observation did not follow the results of the DSC study (Table 1). This might be explained by differences in both the content of 'soft' phase, i.e. swollen PEG phase, and in the degree of swelling of the PEG phase. Consequently, membrane PEG85-2 had the highest content of mechanically 'soft' phase, but this PEG phase had the lowest degree of swelling. On the other hand, membrane PEG70-2 had the lowest content of 'soft' phase, but contained the most swollen PEG phase. In the temperature region of the glass transition temperature of the 'soft' phase, the DSC measured the thermal properties of the plasticized PEG phases and, as discussed above, the T_g was found to decrease with degree of swelling. In the same temperature region, DMA measured the mechanical properties of the entire membranes, and the temperature of tan δ_{max} was found to decrease with the content of the 'soft' phase. In agreement with the DSC study, the position of tan δ_{max} moved toward higher temperatures when the degree of crosslinking of the PEG phase was increased, see Fig. 7(b). As seen in Fig. 7(c), a large effect on tan δ was observed when the salt concentration of the electrolyte solution was varied in the membranes. The temperature of tan δ_{max} shifted only slightly when the concentration was increased from 0.5 to 1.0 M LiTFSI in γ-BL. However, when the salt concentration was increased further, the temperature of tan δ_{max} increased significantly. Thus, an increase in the salt concentration from 0.5 to 2.0 M brought an increase in the temperature of tan δ_{max} from −90 to −55 °C.

As expected, the gel membranes in the present study exhibited a gel-like behavior, that is $E' > E''$ [35]. The higher the value of tan δ, the more viscous is the material. The degree of crosslinking had the largest impact on the value of the tan δ_{max}, as seen in Fig. 7(b). An increase in the amount of PEG400diMA in the PEG macromonomer mixture of the dry solid membranes gave a lower value of tan δ for the corresponding gel membranes, and thus indicated that the membranes were less 'liquid-like'. The data of tan δ as a function of temperature may be analyzed to study the heterogenity of the samples [18]. In our previous

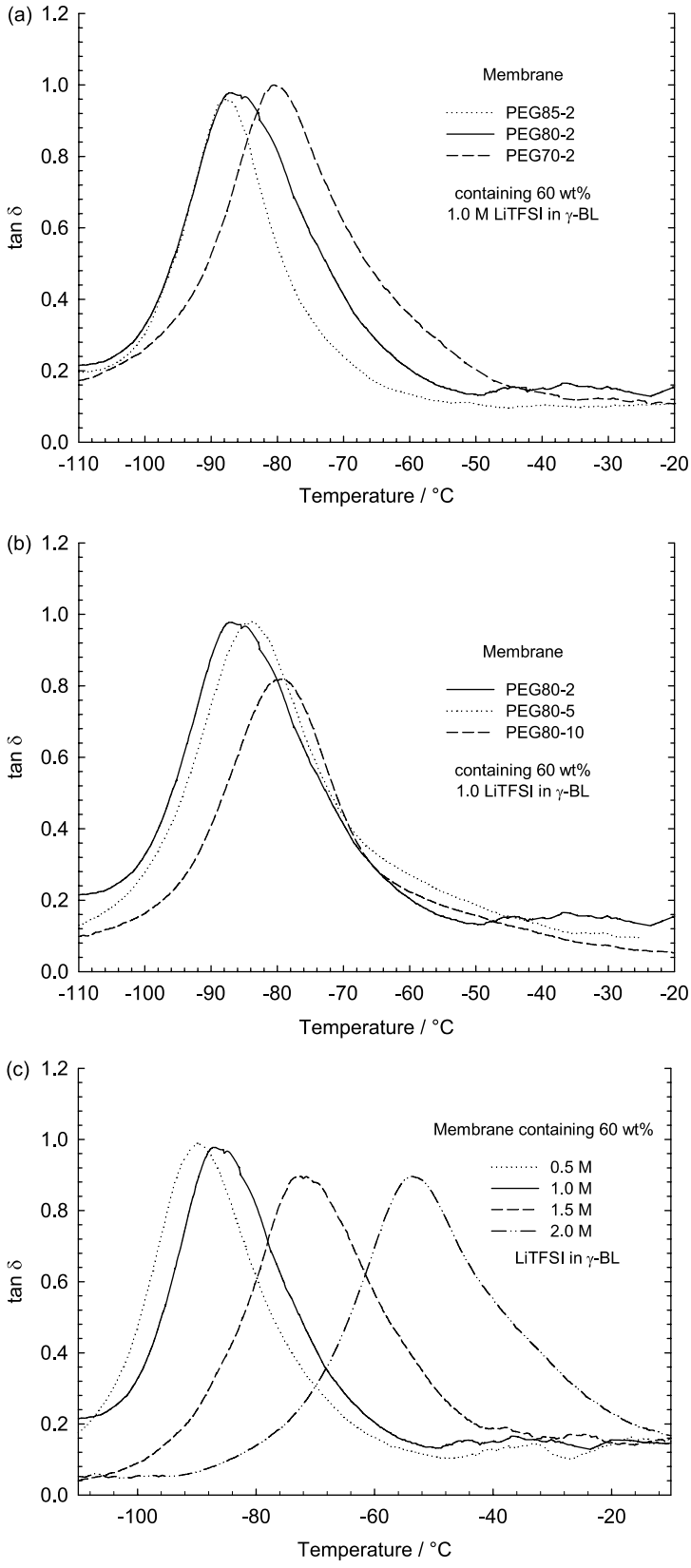

Fig. 7. Tan δ curves for gel membranes with (a) varying PEG content, (b) varying degree of crosslinking of the PEG phase and (c) varying LiTFSI salt concentration in the membranes based on PEG80-2. In all cases, the membranes contained 60 wt% electrolyte solution.

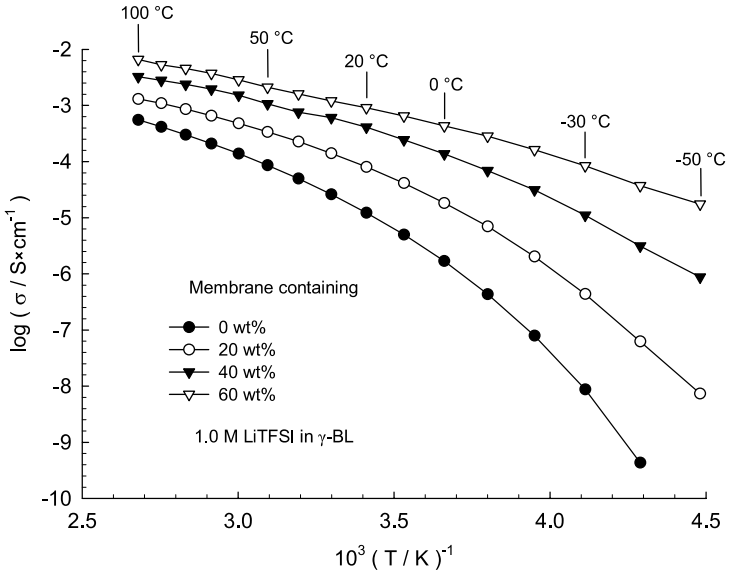

Fig. 8. Arrhenius conductivity plots for gel membranes with content of electrolyte solution. The gel membranes were prepared from membrane PEG80-2.

study, it was observed that the width of the tan δ peaks in the mechanical spectra of the solid membranes varied. A broadening appeared as a high temperature shoulder of the peak and the broadening increased with decreasing contents of PEG phase and decreasing degree of crosslinking. It was proposed that this shoulder originated from an amorphous blend phase of PEG-grafted polymethacrylate and PVDF–HFP [18]. In the present study, a careful inspection of the results presented in Fig. 7(a) and (b) revealed a slight tendency for a similar broadening with increasing amount of PVDF–HFP and decreasing degree of crosslinking, respectively. A broadening of the high temperature shoulder of the tan δ curve was clearly noted as the LiTFSI salt concentration was increased, see Fig. 7(c). This was especially pronounced for the membranes containing 60 wt% of 1.5 and 2.0 M LiTFSI in γ-BL.

3.6. Conductivity measurements

The conductivities of the gel electrolytes were evaluated by EIS, and studied as a function of PEG phase content, degree of crosslinking, liquid content, and salt concentration for the different membranes. Fig. 8 shows the conductivity of the membranes containing between 0 and 60 wt% of 1 M LiTFSI in γ-BL. As expected, the level of conductivity increased considerably as the dry membranes were swollen with the electrolyte solution. For example, at 20 °C the conductivity was approximately 10^{-5} and 10^{-3} S cm^{-1} for the membranes containing 0 and 60 wt%, respectively, of the electrolyte solution. The conductivities of the solid, dry membranes have previously been reported to follow the Vogel–Tammann–Fulcher (VTF) equation, which was indicated by a positive curvature of the Arrhenius plots

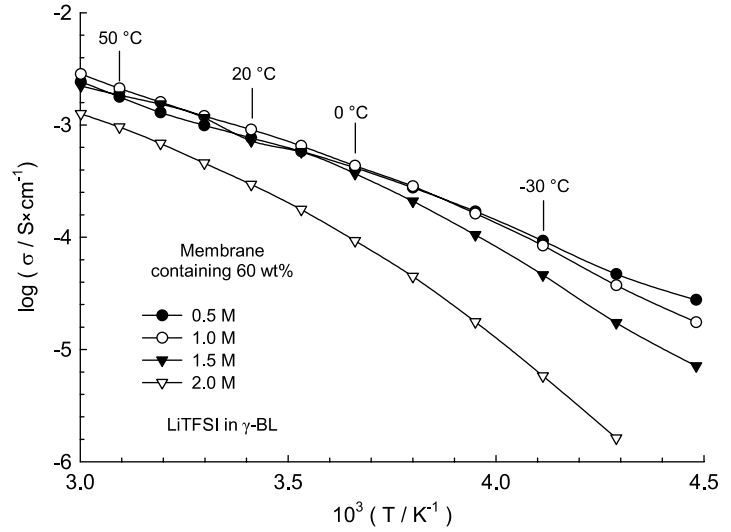

Fig. 9. Arrhenius conductivity plots for gel membranes with varying LiTFSI salt concentration. The gel membranes were prepared from membrane PEG80-2.

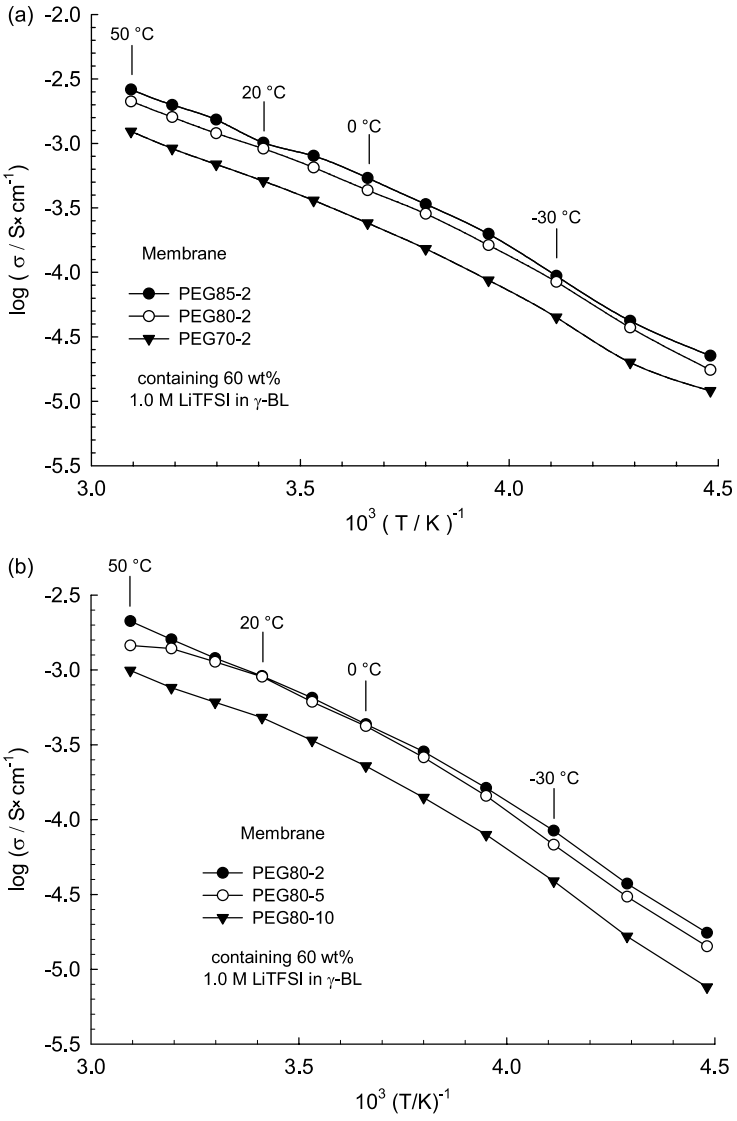

Fig. 10. Arrhenius conductivity plots for gel membranes with (a) varying PEG phase content and (b) varying degree of crosslinking.

[18]. This implied that the conduction mechanism was linked to the segmental mobility of the PEG phase. The Arrhenius plots in Fig. 8 revealed that the conduction mechanism became increasingly coupled with the dynamics of the solvent, and consequently less coupled to the segmental motion of the PEG-grafted polymethacrylate, as the level of solvent content was increased. This was indicated by the more linear shape of the conductivity curves of the highly swollen membranes.

Fig. 9 shows Arrhenius plots of the conductivity of membranes containing 60 wt% of electrolyte solutions with salt concentrations between 0.5 and 2.0 M. At low temperatures, the membrane with the highest salt concentration showed the lowest level of conductivity. The DSC analysis showed that higher salt concentrations brought increases in the T_g as the level of ionic interactions in the swollen PEG phase increased. As the temperature was increased, the difference between the conductivities decreased as the conductivity of the membranes with the high salt concentrations increased faster than the membranes containing low salt concentrations. The likely reason for this observation was that, as $T-T_g$ increased, the difference in the segmental mobility became less pronounced, and number of charge carriers became increasingly important for the conductivity. The optimum salt concentration of the electrolyte solution at 20 °C seemed to be approximately 1 M, at least for the membranes containing 60 wt% of electrolyte solution. At higher salt concentrations the conductivity decreased, possibly by the combined effect of ion aggregation and increasing values of T_g, as indicated by the DSC, IR, and DMA studies.

Fig. 10(a) shows the influence of different amounts of PEG in membranes containing 60 wt% electrolyte solutions. The membrane containing the highest amount of PEG had the highest conductivity. As mentioned above, this membrane contained the highest content of ‘soft’

conducting phase, i.e. swollen PEG-grafted polymethacrylate, but simultaneously had the lowest degree of swelling of this phase. In the present case, the overall content of conducting phase was seemingly more important for the conductivity than the degree of swelling of the PEG phase. The degree of crosslinking within the PEG phase also influenced the ionic conductivity of the gel membranes, as shown in Fig. 10(b). The conductivity did not vary significantly as long as the degree of crosslinking was kept at a low degree, as for the gel membranes based on dry membranes prepared with 2 or 5 wt% PEG400diMA in the monomer mixture. However, a clear decrease in the conductivity was observed when the degree of crosslinking was increased above this level. The same general observation was made in the study of the dry solid polymer electrolyte membranes [18].

The highest conductivity at 40 °C, approximately 1.6×10^{-3} S cm^{-1}, was reached by membrane PEG85-2 containing 60 wt% of 1 M LiTFSI in γ-BL. This value may be compared to the conductivities obtained with gel electrolytes based on porous PVDF–HFP membranes [36] or crosslinked PEG structures [37,38]. Both these electrolyte systems have been reported to reach conductivities in the range 2.5×10^{-4} to 3.2×10^{-3} S cm^{-1} at 40 °C when containing comparable levels of liquid electrolytes as used in the present study. The level of conductivity of PVDF–HFP–PEG gel electrolytes are generally found to be related to the porosity of the PVDF–HFP phase and the degree of crosslinking within the PEG-containing phase, respectively. Polymer gel electrolytes based on PVDF–HFP and PEG have previously been studied by Cheng et al. [39]. With the aim to mechanically reinforce the membranes, they prepared microporous polymer blends composed of PVDF–HFP, PEG400diMA and free PEG400. After thermal curing of the dimethacrylate oligomer, these blends were allowed to take up different amounts of 1 M $LiPF_6$ in a mixture of ethylene carbonate:diethylene carbonate (1:1, v:v). Gel electrolytes containing 40 wt% of liquid electrolyte showed conductivities of 3.2×10^{-4} S cm^{-1} at 40 °C, which was half a decade below the conductivity of the present electrolyte membranes containing 40 wt% electrolyte solution. However, the samples prepared in the study by Cheng et al. had a PVDF–HFP:PEG ratio of 1:1 (wt:wt) and a different membrane morphology, as compared the membranes of the present study.

4. Conclusions

Self-supporting gel membranes were prepared by allowing dry solid polymer blend membranes to take up controlled amounts of γ-BL containing LiTFSI salt. The solid membranes consisted of co-continuous blends of PVDF–HFP and PEG-grafted polymethacrylate. The PEG phase imbibed the major part of the liquid electrolyte, and the Li^+ ions were found by FTIR spectroscopy to preferentially interact with the ether oxygens of the PEG. The three-dimensional matrix of PVDF–HFP in the membranes was seemingly unaffected by the solvent uptake and retained the mechanical stability of the gel membranes. The LiTFSI salt concentration of the electrolyte solution had the largest influence on the properties of these gel membranes. The highest ionic conductivity in the present study, just above 10^{-3} S cm^{-1} at 20 °C, was achieved when the membranes contained 60 wt% of 1.0 M LiTFSI in γ-BL. This study points towards an attractive concept to combine high ionic conductivity with mechanical stability in polymer gel electrolyte membranes.

References

[1] Watanabe M, Kanba M, Nagaoka K, Shinohara I. J Polym Sci, Polym Phys Ed 1983;21:939.
[2] Choe HS, Carroll BG, Pasquariello DM, Abraham KM. Chem Mater 1997;9:369.
[3] Bohnke O, Rousselot C, Gillet PA, Truche C. J Electrochem Soc 1992;139:1862.
[4] Choe HS, Giaccai J, Alamgir M, Abraham KM. Electrochim Acta 1995;40:2289.
[5] Choi Y, Kim S, Chang K. J Appl Electrochem 1997;27:1118.
[6] Reiche A, Sandner R, Weinkauf A, Sandner B, Fleischer G, Rittig F. Polymer 2000;41:3821.
[7] Aihara Y, Appetecchi GB, Scrosati B. J Electrochem Soc 2002;149: A849.
[8] Liu HJ, Hwang JJ, Chen-Yang YW. J Polym Sci, Part A: Polym Chem 2002;40:3873.
[9] Boudin F, Andrieu X, Jehoulet C, Olsen II. J Power Sources 1999;81–82:804.
[10] Huang H, Wunder SL. J Power Sources 2001;97–98:649.
[11] Magistris A, Mustarelli P, Parazzoli F, Quartarone E, Piaggio P, Bottino A. J Power Sources 2001;97–98:657.
[12] Appetecchi GB, Croce F, De Paolis A, Scrosati B. J Electroanal Chem 1999;463:248.
[13] Song JM, Kang HR, Kim SW, Lee WM, Kim HT. Electrochim Acta 2003;48:1339.
[14] Wang H, Huang H, Wunder SL. J Electrochem Soc 2000;147:2853.
[15] Kim DW, Oh B, Park JH, Sun YK. Solid State Ionics 2000;138:41.
[16] Kim DW, Noh KA, Chun JH, Kim SH, Ko JM. Solid State Ionics 2001;144:329.
[17] Gavelin P, Jannasch P, Wesslen B. J Polym Sci, Part A: Polym Chem 2001;39:2223.
[18] Munch Elmer A, Wesslen B, Sommer-Larsen P, West K, Hassander H, Jannasch P. J Mater Chem 2003;13:2168.
[19] Abbrent S, Plestil J, Hlavata D, Lindgren J, Tegenfeldt J, Wendsjö Å. Polymer 2001;42:107.
[20] Richards EG. An introduction to physical properties of large molecules in solution. Cambridge, UK: Cambridge University Press; 1980.
[21] Tanaka T, Fillmore DJ. J Chem Phys 1979;70:1214.
[22] Caillon-Caravanier M, Claude-Montigny B, Lemordant D, Bosser G. J Power Sources 2002;107:125.
[23] Hayamizu K, Aihara Y, Arai S, Price WS. Solid State Ionics 1998; 197:1.
[24] Hayamizu K, Aihara Y, Arai S, Price WS. Electrochim Acta 2000;45: 1313.
[25] Forsyth M, Carcia M, MacFarlane DR, Ng S, Smith ME, Strange JE. Solid State Ionics 1996;86–88:1365.
[26] Kobayashi N, Sunaga S, Hirohashi R. Polymer 1992;33:3044.

[27] Kim CS, Oh SM. Electrochim Acta 2001;46:1323.
[28] Cho JW, Song HY, Kim SY. Polymer 1993;34:1024.
[29] Kynar PVDF for Lithium Batteries, Technical Brochure, Elf Atochem, ATO.
[30] Burell H. In: Branderup J, Immergut EH, editors. Polymer handbook. 2nd ed. New York: Wiley Interscience; 1974 [chapter IV.15].
[31] Jannasch P. Polymer 2001;42:8629.
[32] Brouillette D, Perron G, Desnoyers JE. J Solution Chem 1998;27:151.
[33] Gavelin P, Ostrovskii O, Adebahr J, Jannasch P, Wesslen B. J Polym Sci, Part B: Polym Phys 2001;39:1519.
[34] Aihara Y, Arai S, Hayamizu K. Electrochim Acta 2000;45:1321.
[35] Almdal K, Dyre J, Hvidt S, Kramer O. Polym Gels Networks 1993;1:5.
[36] Zhang SS, Xu K, Foster DL, Ervin MH, Jow TR. J Power Sources 2004;125:114.
[37] Abbrent S, Lindgren J, Tegenfeldt J, Wendsjö Å. Electrochim Acta 1998;43:1185.
[38] Kang YK, Cheong K, Noh KA, Lee C, Seung DY. J Power Sources 2003;119:432.
[39] Cheng CL, Wan CC, Wang YY. Electrochem Commun 2004;6:531.